

A&A manuscript no.
(will be inserted by hand later)

Your thesaurus codes are:
08(08.01.1;08.05.1;08.23.2;09.01.1;13.07.2)

ASTRONOMY
AND
ASTROPHYSICS

Modelling Radioactivities and other Observables from OB Associations

Stefan Plüschke¹, Roland Diehl¹, Dieter H. Hartmann², and Uwe G. Oberlack³

¹ MPI für extraterrestrische Physik, Giessenbachstrasse, D-85740 Garching, Germany

² Department of Physics and Astronomy, Clemson University, Clemson, SC 29634, USA

³ Astrophysics Laboratory, Columbia University, New York, NY 10027, USA

Received (May 10 2000)/ Accepted (???)

Abstract. Recent observations of the diffuse Galactic gamma-ray glow at 1.809 MeV, attributed to the radioactive decay of ²⁶Al, point towards a massive star origin of this radioactive isotope. Wolf Rayet stars and core-collapse supernovae appear to dominate the production of this isotope. Massive stars are commonly located in clusters and OB associations, regions of recent star formation. We thus discuss the temporal evolution of ²⁶Al, and ⁶⁰Fe within evolving OB associations. The goal of this study is to utilize the associated gamma-ray lines as a diagnostic tool for the study of correlated star formation, and also to provide more detailed models for the interpretation of data obtained with COMPTEL on the Compton Observatory. We investigate the effects of possible aluminum yield enhancements, predicted for some massive close binary systems. In addition to the ejection of chemically processed matter, massive stars also drive strong stellar winds and emit large fluxes of ionizing radiation. This energy and radiation input into the interstellar medium (ISM) is crucial for the dynamical evolution of the gas and subsequent star forming activity in the galactic disk. We discuss population synthesis models for a variety of star formation histories, and compare the predicted gamma-ray line lightcurves to COMPTEL measurements in the Cygnus region. Radioactive tracers such as ²⁶Al and ⁶⁰Fe provide a unique gamma-ray tracer of Galactic star formation activity, complementary to other methods using spectral information in the radio, IR or optical bands.

Key words: stars: abundances, early-type, associations – ISM:abundances – γ -rays: observations

1. Introduction

For almost a decade the COMPTEL instrument aboard the Compton Observatory (Schoenfelder et al. 1993) has mapped the diffuse Galactic emission in the 1.809 MeV line (Diehl et al. 1995, Oberlack et al. 1996, and Plüschke et al. 1999a). This gamma-ray line is believed to be due to the decay of radioactive ²⁶Al, which can be produced in

many different environments. One of the primary issues in the interpretation of this map is the identification of the dominant source of this isotope. Several studies of correlations between the 1.8 MeV map and diffuse maps taken in low energy bands suggest that the gamma-ray patterns follow closely those of the massive star population (Prantzos & Diehl 1996, Diehl & Timmes 1998, Knödseder et al. 1999). In particular, Knödseder et al. (1999) recently demonstrated that the 1.809 MeV emission profile correlates best with electron bremsstrahlung emission in the microwave regime, which traces the free electrons which in turn are produced by the ionizing radiation from massive stars. The gamma-ray line from ²⁶Al thus appears to directly trace the presence of massive stars, so that Wolf Rayet stars and core-collapse supernovae emerge as the most promising source candidates (Prantzos & Diehl 1996). With a typical stellar yield of $10^{-4}M_{\odot}$ of ²⁶Al injected into the ISM per massive star (during the WR phase and in the supernova event) and a million year lifetime, one expects a steady state amount of $\sim 1 M_{\odot}$ of radioactive aluminum in the ISM at any time. Spread throughout the disk of the Galaxy this amount can explain the observed diffuse 1.8 MeV line flux.

In addition to the nucleosynthesis of radioactive matter, which traces the evolution over the past few million years, massive stars dynamically shape the interstellar medium on a similar time-scale (e.g., Lozinskaya 1992). Due to their high mass loss rates (Barlow et al. 1981, de Jager 1988) and large wind velocities (Cassinelli & Lamers 1987), massive stars impart a large amount of momentum and kinetic energy to the surrounding medium (e.g., van der Hucht et al. 1987; Leitherer et al. 1992). Due to their large surface temperatures, massive stars also emit a large fraction of their radiative luminosity in the wavelength regime below 91.2 nm, causing photoionization of the surrounding medium (e.g., Panagia 1973, Vacca et al. 1996). The subsequent supernova explosions contribute additional energy (typically 10^{51} erg (Jones et al. 1998, and references therein)), although much of this energy might be radiatively lost (Thornton et al. 1998), as well as fresh products of stellar

nucleosynthesis.

In a population synthesis approach we compute the light-curves of ^{26}Al (and also ^{60}Fe) together with the mechanical and extreme ultra-violet luminosities as a function of time for different star formation histories. ^{26}Al and ^{60}Fe yields are taken from recent WR models (Meynet et al. 1997) and supernova simulations (Woosley & Weaver 1995; Woosley et al. 1995). We also study the potentially important role of yield enhancements for stars that are members of particular binary systems (Langer et al. 1998). For an assumed star formation history the corresponding gamma-ray line flux then provides a unique diagnostic tool to study star forming regions, complementing other tracers such as IR, UV, or $\text{H}\alpha$ emission. We use the gamma-ray light curves to constrain the star formation history of the the Cygnus region, which is one of the brightest isolated features in COMPTEL's 1.809 MeV map.

The paper is organized as follows. In section 2 we review the COMPTEL 1.8 MeV results. In section 3 we construct an OB association model based on three major aspects; nucleosynthesis of radioactive matter, injection of kinetic energy, and emission of extreme ultra violet radiation. We contrast results from a starburst with those from a continuous star formation history. A comparison with recent COMPTEL observations of the Cygnus region is presented in section 4. We present our conclusions in section 5.

2. The 1.8 MeV Sky and the Cygnus Region

The early COMPTEL 1.809 MeV images (Diehl et al. 1995) immediately led to a lively discussion about the dominant sources of galactic ^{26}Al . Radioactive ^{26}Al is produced during hydrostatic H-burning in the cores and shells of massive stars (Meynet et al. 1997), in hydrostatic H-shell-burning, in the so-called hot bottom burning (HBB) in massive AGB stars (e.g., Bazan et al. 1993), during hydrostatic Ne-shell-burning in pre-supernova stars, in explosive H- and Ne-burning in novae (e.g., Jose et al. 1999), and core-collapse supernovae (Woosley & Weaver 1995; Woosley et al. 1995; Thielemann, Nomoto & Hashimoto 1996; Woosley & Heger 1999). The contributions to aluminum in the ISM from AGB stars, novae, and supernovae should lead to different angular patterns of the 1.809 MeV flux, thus in principal allowing a quantitative resolution of the flux into the various source populations (see Clayton & Leising 1987, and Prantzos & Diehl 1996 for a discussion of this method). The COMPTEL Team recently published an updated map, based on 8 years of data (Plüschke et al. 1999a), which confirms the previously reported characteristics of the galactic 1.8 MeV emission; a strong, extended galactic ridge, concentrated towards the inner galaxy, a peculiar emission feature in the Cygnus region (see Fig. 1), and a low-intensity ridge extending to-

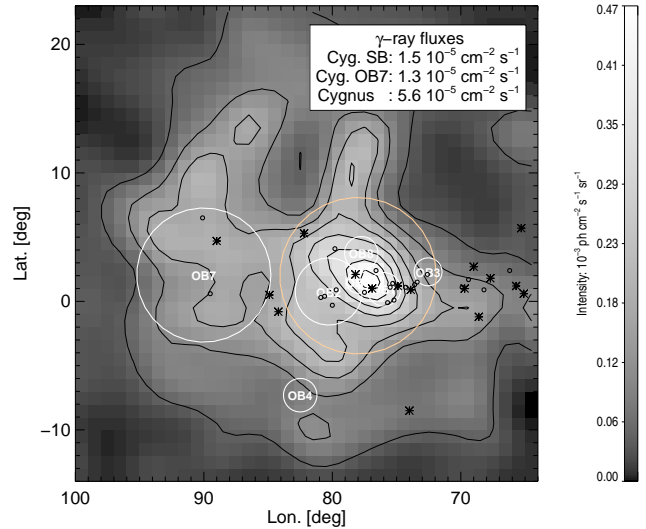


Fig. 1. Maximum Entropy image of the 1.8 MeV gamma-ray line emission due to the decay of ^{26}Al in the Cygnus region, based on 8 years of COMPTEL observations. The contours and colors give the measured γ -ray intensity in the line. Over-plotted are known Wolf Rayet stars (dots), supernova remnants (stars) and OB associations (circles).

towards Carina and Vela. The emerging picture is that massive stars and their subsequent supernovae appear to be the most promising source candidates (Prantzos & Diehl 1996). Recently, Knödseder et al. (1999) carried out an extensive comparison between the 1.8 MeV map and a variety of other tracers of star formation activity such as CO emission, dust maps, and secondary indicators of ionization (e.g. electron free-free emission). These comparisons strongly support a correlation between massive stars and 1.8 MeV emission. Early-type stars are predominantly found in regions of recent star formation, so that we can test the global correlation with a detailed analysis of the Cygnus star forming region. Fig. 1 is an enlarged image of this region drawn from the COMPTEL 1.8 MeV survey. Due to their high mass loss rates Wolf Rayet stars and core-collapse supernovae are primary candidates for ^{26}Al sources. In Fig. 1 Wolf Rayet stars and supernova remnants are marked by dots and stars, respectively. The encircled regions mark identified OB associations in the Cygnus complex. The Cygnus region includes at least 21 Wolf Rayet stars and 17 supernova remnants, as well as 8 OB associations of different richness class and age.

3. Modelling OB Associations

The Wolf Rayet phase and the core-collapse supernova explosion are specific episodes during the evolution of massive stars. Therefore groups and associations of early-type stars are key targets for ^{26}Al abundance studies. Massive stars have a significant dynamic impact on the surrounding interstellar medium, especially when their winds and explosions occur in near- simultaneity. Star formation is

known to occur in groups with a hierarchical size distribution (e.g. Elmegreen, D.M. & Salzer, J.J. 1999, Efremov, Y.N. & Elmegreen, B.G. 1998), ranging from small groups to spiral arm fragments. The mini star-burst leading to group or cluster formation might lead to a coeval population of ZAMS stars, but it might also be spread over some significant span in time. But the subsequent stellar wind and supernova phases are still significantly localized (in space and time), so that the energy input into the ISM from multiple explosions can lead to the formation of super-supernova remnants, commonly referred to as superbubbles (e.g. Tomisaka et al. 1981). We therefore study the properties characterizing the interactions of groups of massive stars with their surrounding medium with a self-consistent population synthesis approach.

Our aim is to establish a numerical model, based on available stellar evolution models (Maeder et al. 1994; Woosley et al. 1993, 1995), of the temporal evolution of a star forming region, with emphasis on gamma-ray line producing isotopes. To achieve a simple and transparent description of the investigated parameters, the model uses a semi-analytic approach. We utilize the detailed models on the basis of simple fit-functions; e.g. power-law description for the stellar lifetime τ_{star} as function of the initial mass M_i . All our simulations start with solar composition, but incorporate subsequent chemical evolution. The inclusion of core-collapse supernovae is based on parameter fits to recent calculations by Woosley & Weaver (1995) and Woosley, Langer & Weaver (1995).

Stellar groups are fundamentally characterized by their initial mass function Φ (IMF) and star formation rate Σ (SFR). We adopt the common assumption that the IMF is time-independent and that the SFR is mass-independent. The model employs a lower mass limit of $8 M_{\odot}$, thus restricting the simulation to stars that end their life in a core-collapse supernova. We adopt a single power-law IMF (eq. 1) with exponent $\Gamma = 1.35$, which is relevant for high mass stars considered here (Kroupa 2000; Scalo 1998). The normalisation constant a_0 was chosen such as to normalize the IMF to unity for the mass range under investigation, so $\Phi(M_i)$ gives the probability of existence of a star with initial mass M_i .

$$\Phi(M_i) = a_0 \cdot M_i^{-(1+\Gamma)} \quad (1)$$

As star formation histories we consider either an instantaneous burst or a continuous, constant star formation rate with an adjustable duration. We verified the simulation through consistency checks against model calculations by Leitherer et al. (1992) and results from the STARBURST99 code (Leitherer et al. 1999). Stellar evolutionary phases of particular relevance in our model are the main sequence/post main sequence phase, the Wolf Rayet phase, and the terminal core-collapse supernova. In the case of ^{26}Al synthesis we furthermore include the effects of the presence of massive close binary systems (MCB). For the calculation of the stellar wind properties we specifi-

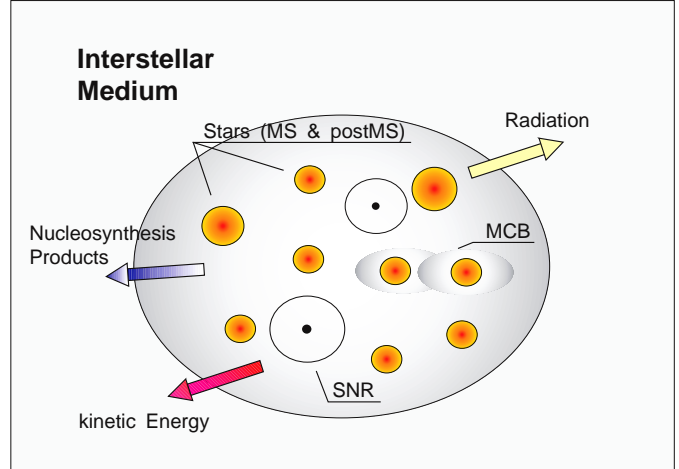


Fig. 2. Schematic overview of the major components of our OB association model.

cally incorporate the BSG/RSG and LBV phases. Fig. 2 provides a schematic overview of the model ingredients. We now describe in greater detail the different processes included in our model, beginning with the ejection of radioactive isotopes with intermediate lifetimes. Then we discuss the description of matter ejection and kinetic energy flux, and present our estimates of the ionizing Lyman continuum emission.

3.1. Synthesis of the Radio-Isotopes ^{26}Al and ^{60}Fe

In addition to ^{26}Al with a mean lifetime of $\tau = 1.04$ Myr and an associated γ -ray line at $E = 1.809$ MeV, we also consider the important radioactivity ^{60}Fe , with a lifetime of 2.07 Myr and comparable yields in core collapse supernovae. ^{60}Fe gives rise to two γ -ray lines in the COMPTEL energy regime at 1.173 MeV and 1.332 MeV. Whereas ^{26}Al can be synthesized in hydrostatic as well as explosive scenarios, explosive nucleosynthesis is the dominant production mechanism for ^{60}Fe (Timmes et al. 1995 and refs therein; Diehl & Timmes 1998). As was emphasized by Timmes et al. ^{26}Al and ^{60}Fe are co-synthesized in the same shells of the collapsing massive star, so the explosive yields of these nuclides are expected to be well correlated. ^{26}Al is produced hydrostatically via proton capture on ^{25}Mg . In this scenario, ^{26}Al is predominately produced during hydrostatic hydrogen burning in cores and shells of massive stars. To be seen by its γ -ray emission, ^{26}Al has to be expelled into the ISM by the star. Thus, effective mixing as well as significant mass loss due to stellar winds are further prerequisites for significant γ -ray emission from hydrostatic ^{26}Al nucleosynthesis. Due to their high mass loss rates, Wolf Rayet stars are expected to be significant contributors to the steady state abundance of ^{26}Al 's in the ISM, and some WR stars are near enough to be potentially detectable as point sources. Fig. 3 shows the ejection rate (mass per unit time) from two representative stars as a function of time. The transition phase of early

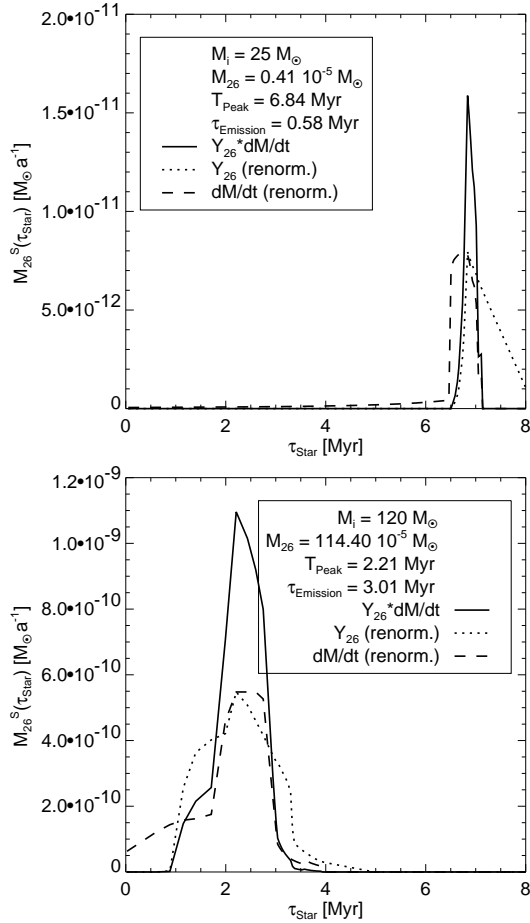


Fig. 3. ^{26}Al emission (in solar masses per year) as a function of time for a $25 M_{\odot}$ (upper panel) and a $120 M_{\odot}$ (lower panel) star.

type stars (Of) towards the post main sequence phases and the early Wolf Rayet phase turn out to be the dominant ejection phases for ^{26}Al . ^{26}Al ejection from AGB stars (Bazan et al. 1993) and nova explosions (Jose et al. 1999) is neglected in this study for two reasons. First, the COMPTEL 1.8 MeV all sky map correlates best with tracers of the young population of massive stars, as discussed in section 2. Second, the timescales involved in AGB and nova phenomena greatly exceed the typical lifetime of OB stars and their associations.

Thus, in modelling ^{26}Al and ^{60}Fe nucleosynthesis in OB associations we focus on contributions from hydrostatic nucleosynthesis of massive stars and explosive synthesis in core-collapse supernovae. Whereas in the case of SNe the ejection of nucleosynthesis products is a singular event in time (eq. 4), the release of hydrostatically produced species by stellar winds has to be treated with a time-dependent model. This is of particular importance for stars for which the duration of ^{26}Al ejection is of the same order, or even much longer, than the lifetime of ^{26}Al . Fig. 3 shows two representative temporal profiles for stars with initial masses of 25 and $120 M_{\odot}$, respec-

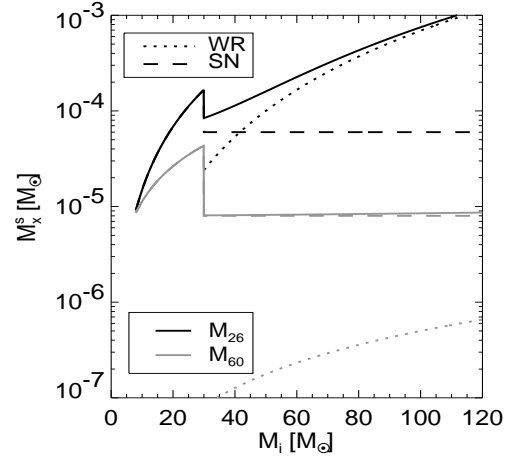


Fig. 4. ^{26}Al and ^{60}Fe lifetime-integrated yields as a function of the stellar mass on the ZAMS.

tively. These profiles are derived from detailed evolutionary models of Maeder & Meynet (1994) and Meynet et al. (1997). To restore the analytic character of the model, we apply a Gaussian approximation (eq. 3) for these profiles. The error of this approximation is less than 10%. The parameters of the Gaussian (area, position and width) are computed on the bases of interpolating polynomials (e.g. $area(M_i) = P_4(M_i)$). Contributions from explosive nucleosynthesis are calculated on the bases of core-collapse supernovae simulations (Woosley & Weaver 1995; Woosley & Heger 1999; Woosley, Langer & Weaver 1995). A direct comparison of explosive yields given in Woosley & Weaver (1995) with results from more recent models including rotation and mass loss (Woosley & Heger 1999) gives good confidence in the older results. Thus we use the yields from the 1995 paper of Woosley & Weaver, covering a wider mass range, to model type II supernovae. Type Ib/c supernovae from more massive stars, showing a Wolf-Rayet phase, are more delicate to incorporate. Woosley, Langer & Weaver (1995) have calculated supernova models for mass losing He stars. Supernova yields presented by this group have to be carefully associated (via the CO core mass (cf. Maeder 1992)) to evolutionary tracks of model stars from Maeder et al. (1994). Unfortunately, these supernova models only cover CO core masses significantly lower than those resulting from mass losing, massive stars ($M_{ZAMS} > 40 M_{\odot}$). On the other hand the CO core masses from the massive stars show only minor variations as function of the initial mass and lie in the range of a $25 M_{\odot}$ star. Thus we decided to model the radio-isotope yields from type Ib/c supernovae by a constant value. Fig. 4 displays the lifetime-integrated $^{26}\text{Al}/^{60}\text{Fe}$ yields as function of the initial mass. In the case of ^{26}Al the integrated yield for stars more massive than $40 M_{\odot}$ is strongly dominated by the wind ejected ^{26}Al . In the case of ^{60}Fe the wind ejected yield is negligible.

To calculate the amount, $M_x(t)$, of radio-nuclides x we

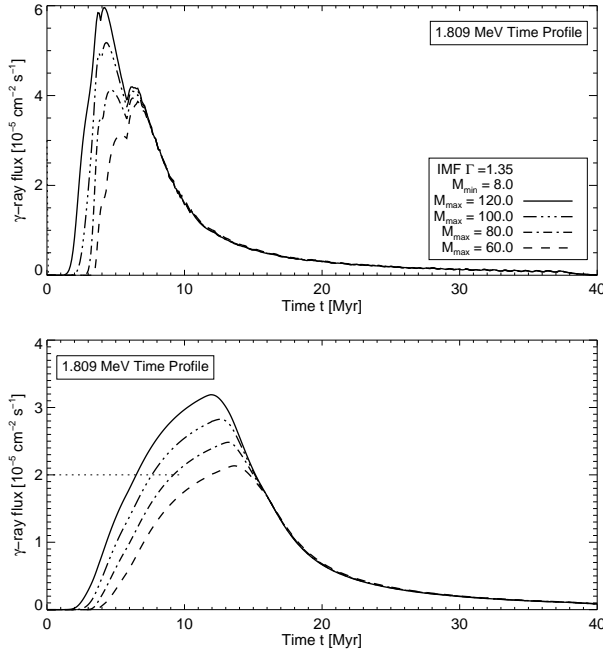


Fig. 5. ^{26}Al lightcurves from an OB association at a distance of 1 kpc in the case of a burst-like star formation converting $10^4 M_\odot$ into stars (upper panel) and a 20 Myr episode of constant star formation rate that forms the same mass of stars (lower panel).

solve equation 2 with the approximations given in equations 3 and 4 (see text above).

$$M_x(t) = \int_{t_0}^t dt \Sigma(\tilde{t}) \int_{M_{min}}^{M_{max}} dM_i \Phi(M_i) \cdot \int_{\tilde{t}}^t d\tilde{t} y_x(M_i, \tilde{t} - \tilde{t}) \cdot \exp\left[-\frac{t - \tilde{t}}{\tau_x}\right] \quad (2)$$

$$y_x^{hyd}(t) = \frac{\hat{y}_x(M_i)}{\sigma(M_i)\sqrt{2\pi}} \cdot \exp\left[-\frac{(t - t_{Peak}(M_i))^2}{2\sigma^2(M_i)}\right] \quad (3)$$

$$y_x^{SN}(t) = \hat{y}_x^{SN}(M_i) \cdot \delta((\tilde{t} - t) - \tau_{star}(M_i)) \quad (4)$$

We calculate $M_{26}(t)$ as well as $M_{60}(t)$ for various sets of initial mass function and star formation rate histories. Fig. 5 and 6 show the resulting ^{26}Al and ^{60}Fe lightcurves for an instantaneous starburst and a case with continuous star formation, respectively. In both cases the total mass of stars created was assumed to be $10^4 M_\odot$, with an IMF exponent of $\Gamma = 1.35$. The duration of the star formation activity in the continuous case was 20 Myr. To convert the resulting decay rate to gamma-ray line fluxes we assumed a nominal distance to the star forming region (OB association) of 1 kpc. Lightcurves are calculated using four different upper mass limits in the IMF; 60, 80, 100, and 120 M_\odot . A comparison of the lightcurves shows a strong dependence of shape on the assumed star formation history. In particular, the double-peaked shape of the burst lightcurve is completely washed out

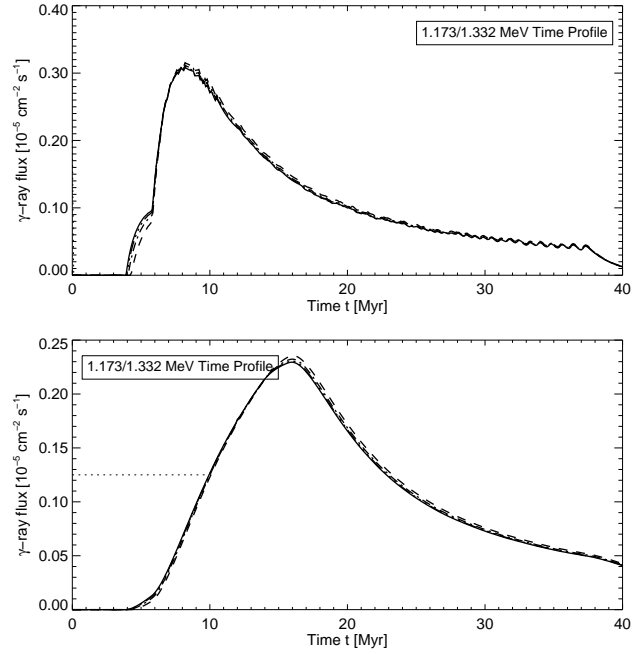


Fig. 6. Same as Fig. 5 for the sum of two high energy γ -ray lines of ^{60}Fe at 1.173 and 1.332 MeV.

in the continuous scenario. Furthermore, peak fluxes are reduced by a significant factor up to 5.

Using COMPTEL's line sensitivity of $10^{-5} \text{ ph cm}^{-2} \text{ s}^{-1}$, we derive upper limits for the detection distances to such regions of star formation: 2.4 kpc at maximum of ^{26}Al for the starburst scenario, and 1.3 kpc in the continuous case, whereas for ^{60}Fe the corresponding values are 1.5 kpc and 1 kpc.

Fig. 7 shows the time-evolution of the ^{60}Fe to ^{26}Al flux ratio. After an initial increase the ratio remains constant at $\sim 10\text{-}20\%$. The increase at late times is due to the vanishing hydrostatic component of ^{26}Al emission and the longer lifetime of ^{60}Fe . In the continuous case associations with an smaller upper mass limit show an increased ratio, due to the suppression of additional ^{26}Al ejection from very massive Wolf Rayet stars. Only during the late phases this ratio increases due to the lifetime difference.

Stars are often observed to form binary systems (Mason et al. 1998). Depending on the relative orbital parameters, mass-transfer reactions via Roche-Lobe overflow (Křiž 1970) may accure. These binary systems are labeled 'close' systems. In massive, close binary systems mass transfer is expected to significantly alter the evolution of the individual stars. These modifications may also induce significant variations in the nucleosynthesis and the subsequent enrichment of the surrounding ISM compared to single stars. Langer et al. (1998) studied ^{26}Al nucleosynthesis in particular massive close binary systems, based on evolutionary models that include mass transfer from

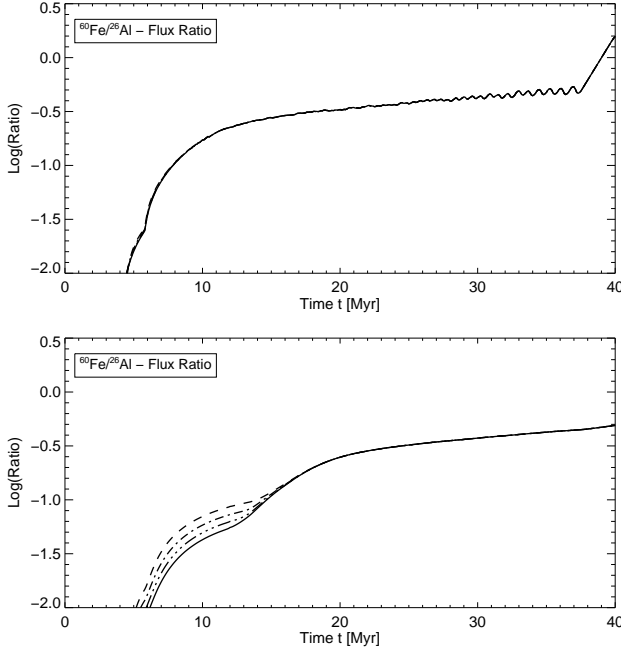


Fig. 7. Flux ratio of ^{60}Fe to ^{26}Al as function of time for a starburst scenario (top) and a continuous star formation (bottom). The ^{60}Fe γ -ray flux is estimated as in Fig. 6.

the primary star. These simulations are still somewhat limited in scope, due to the neglect of stellar winds during the evolution of the massive stars. Furthermore, the calculations were only carried out for quarter solar metallicity. Still, these preliminary investigations strongly suggest that the yield of ^{26}Al can be greatly enhanced during the SN explosion of the secondary, perhaps by as much as a factor 10^3 . The origin of such a large enhancement is attributed to a 'positive interference' of several effects caused by mass-transfer during the main-sequence evolution of the orbiting stars. The models presented by Langer et al. assume case A or case AB mass-transfer, which labels mass-transfer via Roche-Lobe overflow during the core hydrogen burning phase of the primary star (Kippenhahn & Weigert 1967). Due to the loading of fresh material on to the outer layers of the secondary star, the secondary star is rejuvenated. Depending on the details of the mixing processes the opacity of the outer layers of the secondary star is reduced, which causes the mass loss rate to drop significantly. Stars modified in this manner exhibit altered evolutionary tracks (i.e. no WR phase) and end their lives in a supernova explosion as a BSG-like star (similar to SN1987A). Due to the smaller evolutionary gap between the main-sequence and BSG phase, the time-delay between ^{26}Al production and its explosive ejection is drastically reduced. This can lead to a huge enhancement of the yield. The adoption of the modified MCB yields to the framework of our model OB associations, which must rely on solar metallicity models, consequently introduces significant uncertainties.

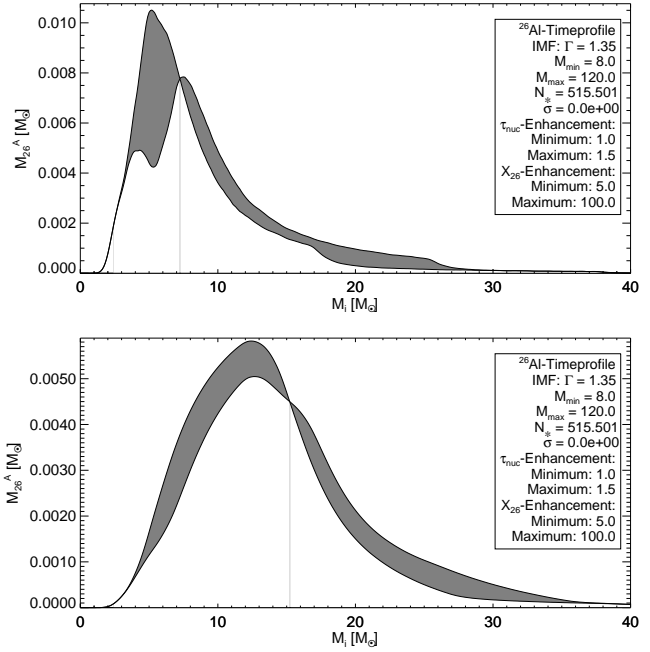


Fig. 8. Ejected ^{26}Al mass as function of time for OB associations with MCB component (top: starburst scenario/ bottom: continuous SF)

For stars of solar metallicity the neglect of stellar winds during the evolution of the individual stars is much more critical than for the case for which Langer et al. worked out their model. We therefore decided on a conservative approach, limiting ^{26}Al yield enhancements to factors less than 10^2 . MCB systems are included in the OB association model with a typical frequency of $\sim 5\%$. This number is based on results of Mason et al. (1998), who finds the total binary frequency in clusters and associations in the solar neighborhood to be at least 59%, while Maeder & Meynet (1994) argued that 8% of such binary systems are massive star systems that undergo a mass transfer phase. We also assumed that all MCB systems show the same enhancement effects. Furthermore, we introduced an upper mass limit for stars in MCB systems in the range 40 to $60 M_{\odot}$. Fig. 8 shows the expelled ^{26}Al mass, $M_{26}(t)$, as a function of time. Except for the additional MCB component all parameters of the simulations are identical to those used in the previous cases. Given the large enhancement factors it comes to no surprise that the M_{26} time profiles are now dominated by the population of MCBs. The SN peak is much more pronounced than in the case of associations consisting exclusively of single stars. In addition, a prolonged evolutionary time in mass-transfer systems causes a time shift that alters the shape of the aluminum profile. The gray shaded area marks the uncertainty due to lifetime variations. Fig. 9 displays the ^{26}Al overproduction due to MCBs, in comparison to a pure single star association that underwent a starburst (keeping the total number

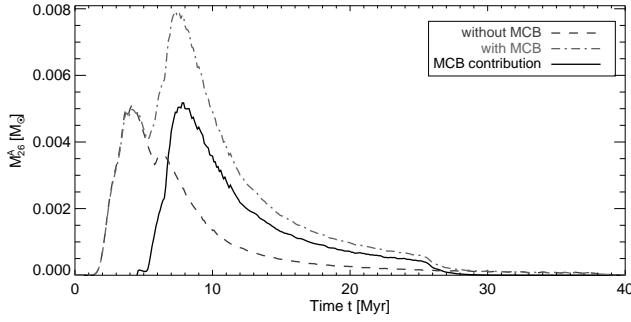


Fig. 9. The gray lines give the ^{26}Al timeprofiles for an upper mass limit of $120 M_{\odot}$ for the two different populations. The black lines show the overproduction of ^{26}Al due to enhanced yields in an association containing MCB systems.

of stars identical in both cases). Due to uncertainties in the MCB implementation, our results for an OB association with an MCB population should be considered preliminary. Further studies of nucleosynthesis in MCB systems that include stellar winds are required to proceed in this investigation.

3.2. Kinetic Energy

Massive stars and supernovae are strong sources of kinetic energy, which significantly affects the dynamics of the surrounding interstellar medium. During the Wolf Rayet phase massive stars experience serious mass loss rates of order $10^{-5} M_{\odot} \text{yr}^{-1}$ (Barlow et al. 1981, Doom 1988, Nugis et al. 1998). This matter is expelled into the surrounding medium with velocities of $\sim 10^3 \text{km s}^{-1}$ (e.g., Prinja et al. 1990). The corresponding mechanical luminosities therefore reach values of order $10^{37} \text{erg s}^{-1}$ for individual Wolf Rayet stars. The contributions from OB stars during the main sequence and red/blue (RSG/BSG) supergiant phase are considerably smaller, due to lower mass loss rates and/or lower wind velocities. The contribution from LBV (luminous blue variables) stars are small as well, due to the short duration of this evolutionary phase. Still, we included these phases in our model. In OB associations continuous energy injection from stellar mass loss coincides with punctuated energy injection from supernovae.

Supernovae typically release 10^{51}erg of energy into the surrounding medium (e.g., Jones et al. 1998). With a supernova rate in the range of 10^{-6} to 10^{-4} per year one thus finds an average mechanical luminosity from SNe that is comparable to that from stellar winds of massive stars.

We adopted mass loss rates given in (Maeder & Meynet 1994) and wind velocities calculated from a fit function provided by Leitherer et al. (1992). For the supernova contribution we assume the standard value of 10^{51}erg per event for all events.

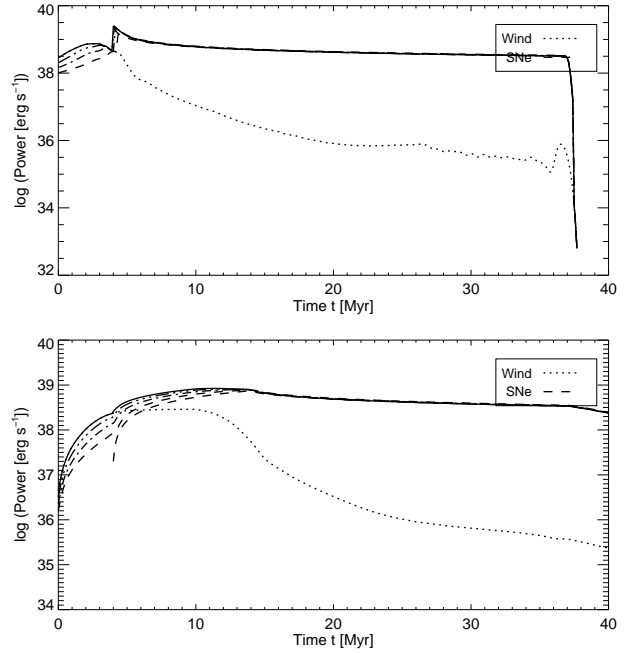


Fig. 10. Timeprofiles of the mechanical luminosity for an OB association in a starburst as well as continuous star formation scenario.

We calculate the timeprofile of mechanical luminosity via equation 5, where l_w is the mechanical wind luminosity of a single star as function of initial mass and age. For two limiting cases (burst vs. continuous star formation) Fig. 10 displays the resulting timeprofiles.

$$L_w(t) = \frac{dN_{stars}(t)}{dt} \cdot 10^{51} \text{erg} + \int_{t_0}^t d\hat{t} \Sigma(\hat{t}) \int_{M_{min}}^{M_{max}} dM_i \Phi(M_i) \cdot \int_{\hat{t}}^t d\tilde{t} l_w(M_i, t - \tilde{t}) \quad (5)$$

$$l_w(M, t) = \frac{1}{2} \cdot \dot{M}(M, t) \cdot v_w^2(M, t) \quad (6)$$

In the starburst scenario the wind and the supernova phase can easily be distinguished. During the early evolution of a burst-formed OB association, stellar winds are the only sources of kinetic energy. Whereas in the later phases supernova events take over and balance the mechanical luminosity near $10^{39} \text{erg s}^{-1}$. In the case of continuous star formation the mechanical luminosity is almost constant over a time period of up to 15 Myr. Then it slightly decreases due to a decrease in the stellar wind contribution.

In addition to the mechanical luminosities we also calculate the total mass loss rate. The mass liberated during the supernova events is determined by assuming that each SN leaves behind a compact remnant with a mass of $1.4 M_{\odot}$. Fig. 11 shows the mass loss rate (integrated over the population) as a function of the age of the association for the two limiting cases of the star formation history. The

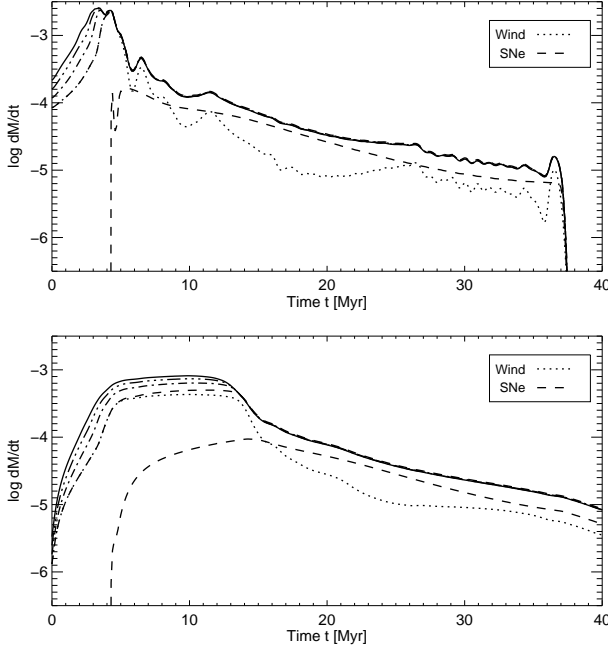


Fig. 11. Mass loss rate of an OB association for a starburst and continuous star formation, respectively.

simulations are based on an identical parameter set to that described in the nucleosynthesis section, but without inclusion of MCB systems. A comparison between stellar wind and supernova mass expulsion shows that the stellar wind is the dominant source of matter blown into the ISM. However, one should keep in mind that ejecta processed in a supernova are more metal enriched than the matter ejected by stellar winds. Thus, supernovae will always increase the metallicity of the surrounding medium.

3.3. Lyman Continuum Emission

Besides the mechanical energy, massive stars also release a large amount of energy in the form of radiation. Due to their high effective temperatures ($\sim 10^4\text{K}$) O stars (e.g. see Maeder & Meynet 1994) emit a significant portion of their electromagnetic radiation in the wavelength regime below $\lambda = 91.2\text{ nm}$ where hydrogen, the by far most abundant element in the interstellar medium, is photoionized. We included this ionizing radiation in our model by fitting the stellar Lyman photon fluxes estimated by Vacca et al. 1996. The adopted fit-function (eq. 7) is accurate within 5% for the whole mass range.

$$Q_{0/1}(M_i) = \exp\left(a_1 + \frac{a_2}{M_i}\right) \cdot 10^{49} \text{ s}^{-1} \quad (7)$$

One major drawback of this approach is the loss of spectral information. We only compute the number intensity of photons capable of ionizing hydrogen (Q_0) and helium (Q_1). Fig. 12 shows the logarithmic temporal profiles of

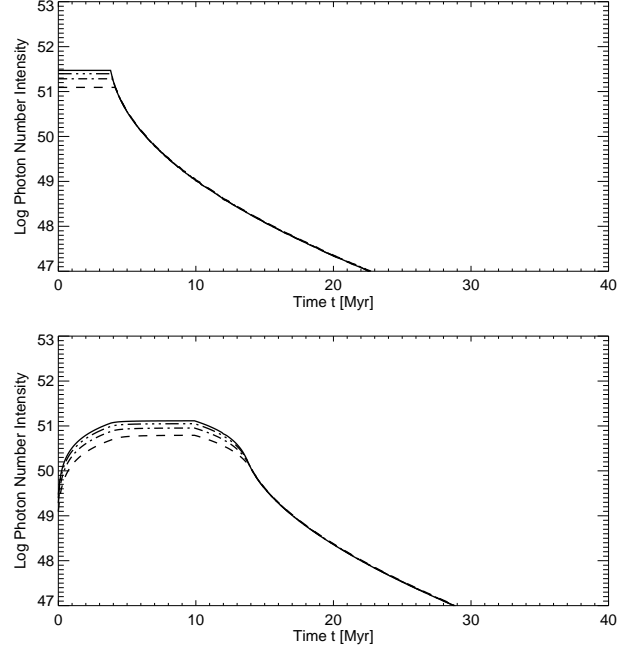


Fig. 12. Timeprofiles of photon number intensity for photons with wavelengths shorter than 91.2 nm.

these integrated EUV-photon fluxes. In the starburst scenario the ionizing flux decreases very quickly, whereas in the case of continuous star formation a plateau phase is quickly reached, and lasts essentially for the whole duration of the star formation activity.

4. ^{26}Al FROM CYGNUS OB ASSOCIATIONS

As mentioned in section 2, the Cygnus region provides a suitable site for a detailed comparison between model predictions and data. Besides the many likely ^{26}Al point sources in this region (Wolf Rayet stars and supernova remnants) Cygnus contains at least 8 OB associations. We use our OB association model to interpret the recent COMPTEL 1.8 MeV results from this field. First results from such a comparison were presented by Plüschke et al. (1999b). In a sub-sequent paper we will summarize our analysis of the Cygnus region in detail, for now we only want to summarize shortly the main results from analysis given in Plüschke et al. (1999b).

On the basis of age and richness estimates by Bochkarev & Sitnik (1985) and Massey et al. (1995) we normalized the IMF by adopting a single power-law with mean exponent $\Gamma = 1.1$ (Massey et al. 1995) (see eq. 1). We then compute ^{26}Al lightcurves for starburst scenarios as well as Gaussian star formation histories with a maximum duration of 15% of the estimated age of the association. The resulting gamma-ray line fluxes have significant uncertainties due to possible variations in the IMF and especially the uncertain MCB contribution. While the model can reproduce the observed flux from the Cygnus region, there is a

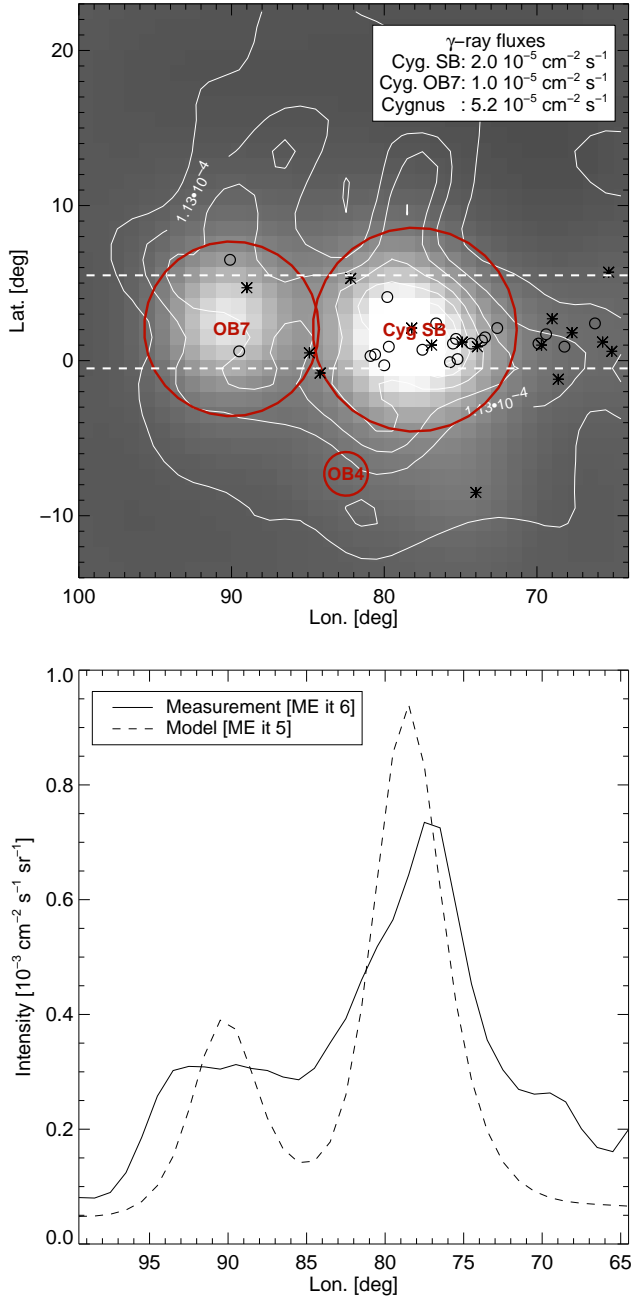


Fig. 13. Model/Measurement comparison for the Cygnus region.

possible variation of a factor ~ 5 , which renders the interpretation somewhat inconclusive. Additional constraints (x-ray flux, dynamic state of the gas in the star forming region, etc) have to be used to improve the model and thus refine the constraints derived from it. Fig. 13 shows a coarse model-measurement comparison. The gray shaded image in the upper panel is a maximum entropy image of a model calculation including MCBs whereas the contour lines mark the COMPTEL maximum entropy result. The lower panel shows a direct comparison of the inten-

sity profiles, taken between the dashed lines in the map. The distributions along the galactic plane are comparable, whereas the reconstructed fluxes are somewhat too low in this example. In future studies we shall incorporate additional diagnostics of the model to refine the analysis of the Cygnus region.

5. SUMMARY & CONCLUSION

We discussed a simple population synthesis model for determining the evolution of the abundance of gamma-ray line producing radioactivity in OB associations. We also traced the stellar output of kinetic/radiative energy and ionizing luminosity, which are essential for studies of the impact of OB associations on the surrounding ISM. A cornerstone of our model is the prediction of emission properties of radioactive isotopes with lifetimes comparable to the main-sequence lifetime of the massive stars that dominate the dynamical evolution of OB association. In particular, we focus attention on ^{26}Al and ^{60}Fe , because the gamma-ray lines from these two species provide a potentially powerful tracer of the star formation history in the association. We advocate the use of gamma-ray line observations as a complementary diagnostic tool. Beside the nucleosynthesis of radioactivities we also model the injection of kinetic energy and extreme ultra-violet radiation. For our future work on the evolution of OB association we plan to use the mechanical luminosity (the central driver) to combine gamma-ray line tracers with a dynamical model for the evolution of a super-bubble, driven by the winds from massive stars and multiple SN events. Based on the results presented here, we draw the following conclusions:

1. Massive stars and their supernovae will give rise to a dynamic evolution with significant temporal variations of the abundances of ^{26}Al and ^{60}Fe . The resulting time profile of the associated gamma-ray lines can be used to constrain or even determine the star formation history of a stellar cluster (OB association).
2. In steady state the ^{60}Fe to ^{26}Al ratio will be of the order 10 - 20% (e.g., Timmes et al. 1995), but in an evolving OB association, this ratio provides an excellent constraint on the age and thus dynamical stage of the system (see Figure 7).
3. MCB systems could dominate the shape of the ^{26}Al lightcurve, but the study of the nucleosynthesis in these systems is not yet mature enough to draw final conclusions.
4. The mass of injected matter into the local interstellar medium due to stellar phenomena is strongly dominated by stellar winds (see Figure 11).
5. The short life-times of early-type stars cause a very rapid decrease of L_{EUV} , so EUV emission is important in very early evolution phases of OB associations. This is also the time when the gamma-ray lines are at detectable levels. It is thus important to consistently treat tracers based on the emitted ionized radiation

and the gamma-ray lines from radioactive aluminum and iron.

6. Detectability of ^{60}Fe : In the 1 MeV regime the narrow line sensitivity of the INTEGRAL spectrometer SPI is expected to be nearly one order of magnitude lower than COMPTEL's sensitivity (for a on-axis observation of 10^6s). Based on the presented analysis of the 1.8 MeV emission of the Cygnus region and the prediction of the flux ratios (see Figure 7), one expects Cygnus to be visible in the ^{60}Fe lines using INTEGRAL.

A comparison of our predictions for ^{26}Al with recent measurements in the Cygnus region shows that our model is capable of reproducing the measured fluxes. On the other hand, the comparison also revealed the need for additional observables to better constrain the models. The inclusion of enhanced aluminum production in MCBs emphasizes the possibility of large uncertainties due to additional free parameters.

The study of star formation in the Galaxy and throughout the universe is a fundamental pillar of modern astrophysics. We know that the global SFR changes by more than an order of magnitude over cosmic time. The Milky Way galaxy also underwent significant evolution of its SF history (though not congruent to that of the universe as a whole), but we do not know the exact shape of the SFR(t) function. We do not even know the exact value of the galaxy wide SFR at the present time, but is of order of a few solar masses per year. We also know that the star formation activity is not spread uniformly though the disk, but instead located in a hierarchy of star forming centers (groups, clusters, associations, complexes, etc., e.g. Elmegreen & Elmegreen 1996). The strong correlations in space and time of the SF process lead to many dynamically active cradles of star formation that in turn drive the dynamics of the ISM and the Galactic disk as a whole. The study of these star forming regions is thus vital to our understanding of galaxy evolution on a larger scale. In this paper we promote the use of gamma-ray lines from radioactive aluminum and iron to study the SF process in these cradles, as well as galaxy wide. The gamma-ray map does not suffer from extinction, so that we get a good global picture of ongoing star formation throughout the Milky Way. Although the flux maps do not contain direct information of distance, realistic spatial models of the emission suggest that the Galaxy indeed converts a few solar masses of gas into stars each year (Timmes et al. 1997). Here we have focused on the Cygnus region to demonstrate how the gamma-ray line method can be applied to individual star forming complexes. The use of radioactive tracers is a relatively recent addition to our arsenal of probes of SF, one that complements other more traditional tools and that should be included in any study of recent star formation activity in the Galaxy. Of course, the life times of the isotopes promoted here limits applications to star forma-

tion within the past 10 Myrs, unless one considers nearby sources.

References

- Barlow, M. J., Smith, L. J. & Willis, A. J., 1981, *MnRAS* 196, 101-110
- Bazan, G., Brown, L., Clayton, D., et al., 1993, *RMxAA* 27, 87
- Bochkarev, N.G. & Sitnik, T.G., 1985, *Ap&SS* 108, 237
- Cassinelli, J.P. & Lamers, H.J.G.L.M.: 1987, Winds from hot young stars. In: *Exploring the Universe with the IUE Satellite*, pp. 139-155
- Clayton, D.D. & Leising, M.D., 1987, *Phys Rep* 144, 1-50
- de Jager, C., Nieuwenhuijzen, H., van der Hucht, K.A., 1988, *A&AS* 72, 259
- Diehl, R., Dupraz, C., Bennett, K., et al., 1995, *A&A* 298, 445
- Diehl, R. & Timmes, F.X., 1998, *PASP* 110, 637
- Doom, C., 1988, *A&A* 192, 170-176
- Efremov, Y.N. & Elmegreen, B.G., 1998, *MNRAS* 299, 643-652
- Elmegreen, B.G., Elmegreen, D.M., Salzer, J.J. & Mann, H. *ApJ* 476, 579-588
- Elmegreen, D.M. & Salzer, J.J., 1999, *AJ* 117, 764-777
- Jones, T.W., Rudnick, L., Jun, B.-I., et al., 1998, *PASP* 110, 125 - 151
- Jose, J., Coc, A., Hernanz, M., 1999, *ApJ* 520, 347
- Kippenhahn, R. & Weigert, A., 1967, *Z. Astrophys.* 65, 251
- Knödseder, J., Bennett, K., Bloemen, H., et al., 1999, *A&A* 344, 68
- Kříž, S. 1970, *Bulletin of the Astronomical Institutes of Czechoslovakia*, 21, 211
- Kroupa, P., 'The Initial Mass Function of Stars', in *Astronomische Gesellschaft Meeting Abstracts*, March 20-24, 2000, talk #11
- Langer, N., Braun, H. & Wellstein, S.: 1998, Massive Close Binaries as Source of galactic ^{26}Al . In: *Proceedings of the 9th Workshop on Nuclear Astrophysics*, Hillebrandt W. & Müller E., MPI f. Astrophysik, Garching, Germany, p. 18
- Leitherer, C., Robert, C., Drissen, L., 1992, *ApJ* 401, 596
- Leitherer, C., Schaerer, D., Goldader, J.D., et al., 1999, *ApJS* 123, 3
- Lozinskaya, T.A., 1992, *Supernovae and stellar wind in the interstellar medium*, published by AIP New York, USA
- Maeder, A., 1992, *A&A* 264, 105-120
- Maeder, A. & Meynet, G., 1994, *A&A* 287, 803
- Mason, B.D., Gies, D.R., Hartkopf, W.I., et al., 1998, *AJ* 115, 821
- Massey, P., Johnson, K.E. & Degioia-Eastwood, K., 1995, *ApJ* 454, 151
- Meynet, G., Arnould, M., Prantzos, N., et al., 1997, *A&A* 320, 460
- Nugis, T., Crowther, P.A. & Willis, A.J., 1998, *A&A* 333, 956-969
- Oberlack, U., Bennett, K., Bloemen, H., et al., 1996, *A&AS* 120, 311
- Oberlack, U., 1997, *PhD Thesis TU Munich*
- Panagia, N., 1973, *AJ* 78, 929-934
- Plüschke, S., Diehl, R., Schönfelder, V., et al.: 1999a, COMPTEL 1.8 MeV All Sky Survey: The Cygnus Region. In: *Proceedings of the 5th COMPTON Symposium*, Ryan J. et al., AIP Conference Proceedings, New York, in press

- Plüschke, S., Diehl, Hartmann, D.H., et al.: 1999b, On the massive Star Origin of ^{26}Al in the Cygnus Region. In: Proceedings of the 5th COMPTON Symposium, Ryan J. et al., AIP Conference Proceedings, New York, in press
- Prantzos, N. & Diehl, R., 1996, Phys. Rep. 267, 1 - 69
- Prinja, R.K., Barlow, M.J. & Howarth, I.D., 1990, ApJ 361, 607
- Scalo, J., in 'The Stellar Initial Mass Function (38th Herstmonceux Conference)', edited by G.Gilmore & D.Howell, 1998, ASP Conference Series, Vol. 142, p. 201
- Schoenfelder, V., Aarts, H., Bennett, K., et al., 1993, ApJS 86, 657-692
- Thielemann, F.-K., Nomoto, K. & Hashimoto, M.-A., 1996, ApJ 460, 408-436
- Thronton, K., Gaudlitz, M., Janka, H.-Th. & Steinmetz, M., 1998, ApJ 500, 95
- Timmes, F.X., Diehl, R. & Hartmann, D.H., 1997, ApJ 479, 760
- Tomisaka, K., Habe, A., & Ikeuchi, S., 1981, Ap&SS 78, 273-285
- Vacca, W.D., Garmany, C.D., Shull, J.M., 1996, ApJ 460, 914
- van der Hucht, K.A., Williams, P.M. & The, P.S, 1987, QJRAS 28, 254-260
- Woosley, S.E. & Heger, A., in 'Astronomy with Radioactivities', MPE Report 274, 1999, ISSN 0178-0719, 133-140
- Woosley, S.E., Langer, N. & Weaver, T.A., 1993, ApJ 411, 823-839
- Woosley, S.E., Langer, N. & Weaver, T.A., 1995, ApJ 448, 315-338
- Woosley, S.E. & Weaver, T.A., 1995, ApJS 101, 181
- Timmes, F.X., Woosley, S.E., Hartmann, D.H., et al., 1995, ApJ 449, 204